RADIO SCIENCE, VOL. 37, NO. 3, 1034, 10.1029/2000RS002613, 2002

A comparison of rain attenuation and drop size distributions measured in Chilbolton and Singapore

Walther Åsen

Norwegian Post and Telecommunications Authority, Oslo, Norway

Chris J. Gibbins

Radio Communications Research Unit, Rutherford Appleton Laboratory, Chilton, Didcot, England, UK

Received 7 February 2001; revised 5 October 2001; accepted 10 October 2001; published 16 May 2002.

[1] Attenuation of radio waves caused by precipitation, especially in the form of rain, is considered to be the limiting factor for new communication systems that will exploit the radio wave spectrum at frequencies higher than about 30 GHz. Over the last 40 years, much effort has gone into theoretical studies characterizing rain in terms of statistical drop size distributions (DSDs), the shapes and velocity dependence of raindrops, and the calculation of raindrop extinction cross sections. This paper focuses on specific data sets and data processing and different ways of viewing DSDs that may help in quantifying some of the important parameters in radio wave propagation from experimental data. Values for the coefficients k and α in the relationship for specific rain attenuation $\gamma = kR^{\alpha}$ are presented, together with rain-rate-dependent parameters for fits of DSDs to standard statistical distributions. These are based on data from Chilbolton, England, and from Singapore. The distributions measured at Chilbolton and Singapore are very different, which strongly suggests that drop size distributions differ under different climatic conditions. Comparisons are also presented of attenuations calculated with values of k and α determined from the DSDs and values found from logarithmic regression between simultaneous rain rate and attenuation measurements at 57, 97, 135, and 210 GHz at Chilbolton. This paper gives a strong indication that the International Telecommunication Union Radiocommunication Sector model for specific rain attenuation is inadequate at frequencies higher than about 70 GHz. *INDEX TERMS:* 3354 Meteorology and Atmospheric Dynamics: Precipitation (1854); 6904 Radio Science: Atmospheric propagation; 6964 Radio Science: Radio wave propagation; *KEYWORDS:* millimeter-wave attenuation, drop size distribution

1. Introduction

[2] The *International Telecommunication Union Radiocommunication Sector* (*ITU-R*) [1997] provides a method to calculate specific rain attenuation from rain rates, which is readily implementable since rain rates are easily obtained and widely available. However, the success of the ITU model depends heavily on the assumptions made about the (local) drop size distributions (DSDs) of the rain. From the early work of *Laws and Parsons* [1943] and *Marshall and Palmer* [1948], much effort has been devoted to characterizing DSDs, often explaining results by characterizing rain events into different categories. Experimental measurements, for example, by *Ugai et al.* [1997], have shown that the general properties of rain drops, such as fall velocities, drop deformations, and fitted statistical shape functions of DSDs, provide an effective understanding. Nevertheless, researchers continue to suggest different parameters for their measured distributions.

[3] From physical principles it may be suggested that a true global DSD cannot exist. The microphysics of clouds and precipitation [e.g., *Rogers and Yau*, 1989] explains the development of raindrops from initial stages as cloud droplets. Because of strong surface tension in very small droplets, a free energy carrier, such as aerosols, must exist in order for condensation of cloud droplets to be possible. Such aerosols can, for instance, be dust particles, salt, or pollution from industry. It is found that a large number of aerosols will create narrow DSDs for cloud droplets, while fewer aerosols tend to

0048-6604/02/2000RS002613

give broader DSDs. Even at latitudes where drops are first formed into ice by ice-forming nuclei, both the varieties and amounts of nuclei will vary between sites. Cloud droplet DSDs are the starting point for drops evolving into precipitation DSDs through coalescence or the ice crystallization process. The next steps in the rain process, with continuing breakup and collisions of raindrops, will of course affect the ability to make exact predictions. Local geography and the available energy in the atmosphere may determine the dimensions of a cumulus cloud. Even so, it seems reasonable to suggest that an initially broad spectrum of droplet diameters will evolve into a resulting broad spectrum of raindrops at the ground. It may therefore be expected that very different DSDs will be found in coastal areas, in very polluted areas, or in areas of very high rainfall rates, where the relative number of aerosol particles is small compared to the total amount of water in the atmosphere. For this reason it is very important to measure DSDs in different areas of the world, which have different climatic conditions and different degrees of, or kinds of, pollution.

[4] It is also useful to fit DSDs to standard mathematical distributions, so that a comparison of parameters for these distributions from different climates can be made in order to facilitate a more general categorization of DSDs, independent of attenuation at particular radio frequencies.

[5] Data for the present study were obtained from a millimeter-wave propagation experiment in southern England, operated by the Rutherford Appleton Laboratory (RAL) for a number of years, in which propagation measurements were made at several frequencies over a short path along which meteorological conditions can be considered as essentially constant. These measurements were supplemented with simultaneous observations of a range of meteorological parameters, including rainfall rates, using rapid response rain gauges, and rain drop size distributions, using an impaxxct-type drop size disdrometer, known as a Joss disdrometer, model RD-69. RAL also operates a rain radar facility situated in Singapore, which includes rain drop size measurements obtained from a colocated impact drop size disdrometer, and data from this experiment have been examined to enable comparisons between rain in different climates.

2. Experiment Setup and Procedures

2.1. Experimental Details

[6] The experimental results for southern England used in this study were obtained on the 500 m Millimetre-Wave Experimental Range at Chilbolton (MWERAC), in Hampshire (57.1°N, 1.4°W, elevation 84 m above mean sea level (amsl)), operated by the Rutherford Appleton Laboratory. The facility and the calibration procedures employed are described in detail by *Gibbins et al.* [1987]. The present work is based on rain attenuation measurements at frequencies of 57, 97, 135, and 210 GHz made at a height of 4 m above the ground (flat grassland) over the 500-m-long line-of-sight link, together with results from an impact-type Joss raindrop size disdrometer, with an active collecting area of 5000 mm^2. The transducer was mounted such that the collecting surface was level with the adjacent ground, to reduce acoustic noise caused by strong winds producing turbulence at the edges of the transducer, which was additionally surrounded with a layer of foam rubber on the ground to reduce splashing from raindrops falling close to the transducer. Data were collected at a sampling rate of 0.1 Hz (integration time 10 s). The data from Singapore were obtained using a similar disdrometer, mounted on top of a building at Nanyang Technological University (1.38°N, 103.7°E, 48 m amsl), with an integration time of 30 s [*Wilson et al.*, 1999].

2.2. Multimodal Distributions and the Calibration of the RD-69 Disdrometer

[7] The multimodal behavior of raindrop size distributions, that is, DSDs with more than one peak, has been studied by many authors. *Steiner and Waldvogel* [1987] have asked the question: ''Is this effect real?'' and answered affirmatively. However, they also pointed out that even very high rainfall rates could not produce equilibrium peaks of coalescence and breakup of drops.

[8] *Jones* [1992] used an automated camera system to measure drop size distributions and found no evidence for such muliple peaks. Nevertheless, he still questioned the statistical significance of his results. The importance of accurate calibration data for the RD-69 disdrometer has been highlighted by *Sheppard* [1990] and by *McFarquhar and List* [1993], who have shown that the multiple peaks of drop size distributions reported by several authors, including G. McFarquhar himself [*List and McFarquhar*, 1990], may be due to fitting of a relationship between drop bin number N (or voltage V) and drop diameter D for the entire valid range of values. In 1990 a more accurate calibration giving 75 calibration points was carried out by Eidgenossische Technische Hochschule (ETH) in Zurich, and the calibration table was published by *McFarquhar and List* [1993]. Figures 1a and 1b show the measured drop size distributions from Chilbolton and Singapore for rain rates in the range 40–50 mm h^{-1}, using the new ETH calibration and the

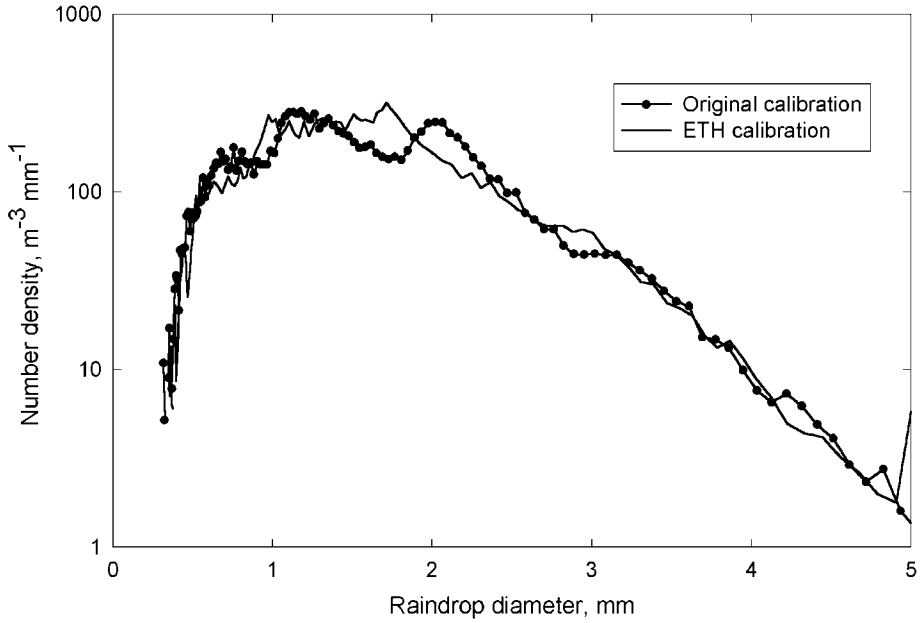

Figure 1a. Drop size density versus drop diameter, for rain rates in the range 40–50 mm h^{-1} (average 45 mm h^{-1}). The curve with circles uses the original manufacturer's calibration for the disdrometer, while the solid curve uses the new ETH calibration. Data are for Chilbolton.

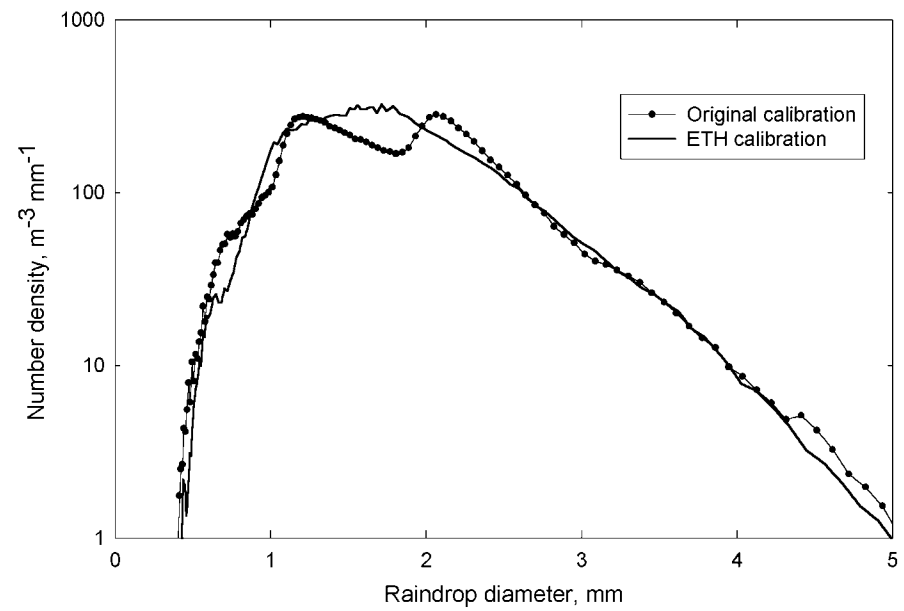

Figure 1b. Drop size density versus drop diameter, for rain rates in the range 40–50 mm h^{-1} (average 45 mm h^{-1}). The curve with circles uses the original manufacturer's calibration for the disdrometer, while the solid curve uses the new ETH calibration. Data are for Singapore.

Table 1. Observations Made at Chilbolton and Singapore in Different Rain Rate Categories

Category Rain Rate, mm h^{-1}	Number of Observations From Singapore	Average Rain Rate at Singapore, mm h^{-1}	Number of Observations From Chilbolton	Average Rain Rate at Chilbolton, mm h^{-1}
0–2	87,304	0.18	1,101,064	0.25
2–4	5085	2.9	47,693	2.8
4–6	2545	4.9	13,380	4.8
6–8	1453	6.9	5038	6.9
8–10	1089	8.9	2188	8.9
10–15	1550	12.2	2147	12.1
15–20	872	17.3	864	17.2
20–25	649	22.4	435	22.3
25–30	534	27.5	287	27.4
30–40	745	34.5	280	34.5
40–50	485	44.7	143	44.9
50–60	316	54.7	91	54.5
60–80	336	68.7	51	66.6
80–90	91	84.5	9	85
90–100	62	95.1	2	99.8
100–110	45	105	1	109.9
110–120	23	114.1		
120–130	9	126.2		
130–140	4	132.8		
140–160	1	145.9		

manufacturer's original calibration. It seems clear that the new calibration removes multiple peaks. The time necessary to reach equilibrium for coalescence and breakup of raindrops is shorter than the total time available from when the drops are created to when they reach the ground, so it was surprising to see the effect of multiple peaks on long-time-averaged distributions. The new ETH calibration has accordingly been used in the present study.

3. Reduction of DSD Data Set

[9] Data for a complete 3-year period from Chilbolton and a 1-year period from Singapore have been averaged and reduced into sets of one matrix and a corresponding vector for each site. The matrix is constructed in the following way: Each row holds the average distribution for a certain category of data, that is, a rain rate interval. The decision about which rain rate category the data belongs to is made after the 10-s integration time for the disdrometer at Chilbolton and after 30 s for the Singapore disdrometer. The rows then hold the average of all DSDs which have rain rates in the different ranges, as given in Table 1. Table 1 also shows the average rain rate to which this corresponds for Chilbolton and Singapore. Figure 2a shows an example of the distributions which have been measured over a 3-year period at Chilbolton, and similarly, Figure 2b shows the 1-year averages for Singapore. The vector holds the number of observations of each rain rate interval, as shown in Table 1.

4. Standard Deviations of Data

[10] Using the same procedure as given in section 3, the standard deviations of DSDs have been determined, together with the standard deviations in the means of the DSD matrices. These give the measured spread of 10-s measurements (or 30-s measurements for the Singapore data) and the measured spread of the 3-year average (and 1-year average for Singapore), respectively. Figures 3a and 3b show examples of the standard deviations and standard deviations in the means for some of the Chilbolton and Singapore DSD data. For the 10-s measurements the standard deviation is of the same order as the average, while the standard deviation of the long-term mean decreases according to the inverse of the square root of the number of observations and becomes very small for a long-term average.

[11] The DSD curves for the higher rain rate categories are smoother for Singapore than for Chilbolton, primarily because there are more data from Singapore at the higher rain rates, as shown in Table 1, and also because each of the observations represents a 30-s average. As expected, the standard deviation of 30-s data (from Singapore) is smaller than the standard deviation of the (Chilbolton) 10-s data.

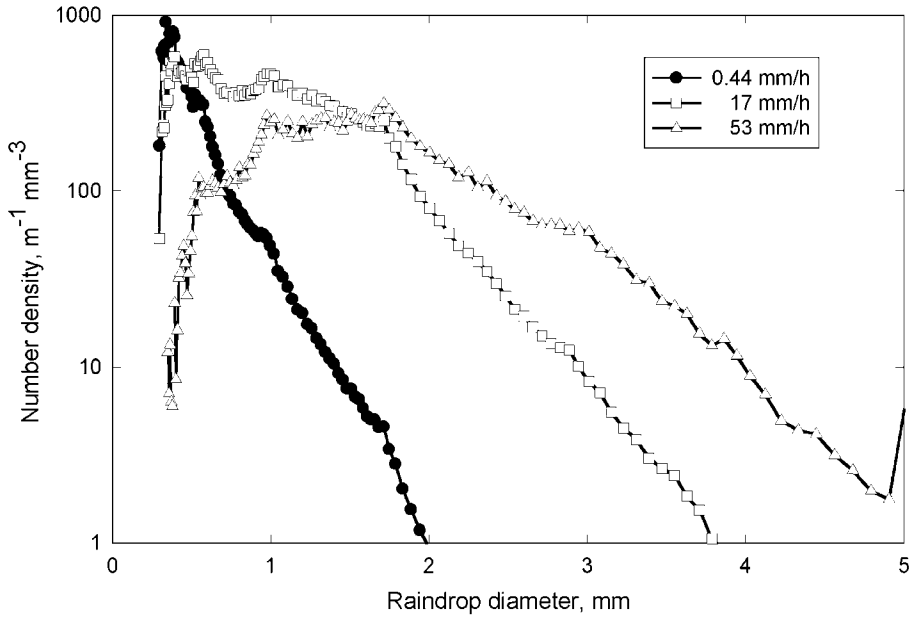

Figure 2a. Drop size density versus drop diameter, for three different categories (0–10, 10–40, and 40–100 mm h^{-1}) of rain rate. The data are from Chilbolton.

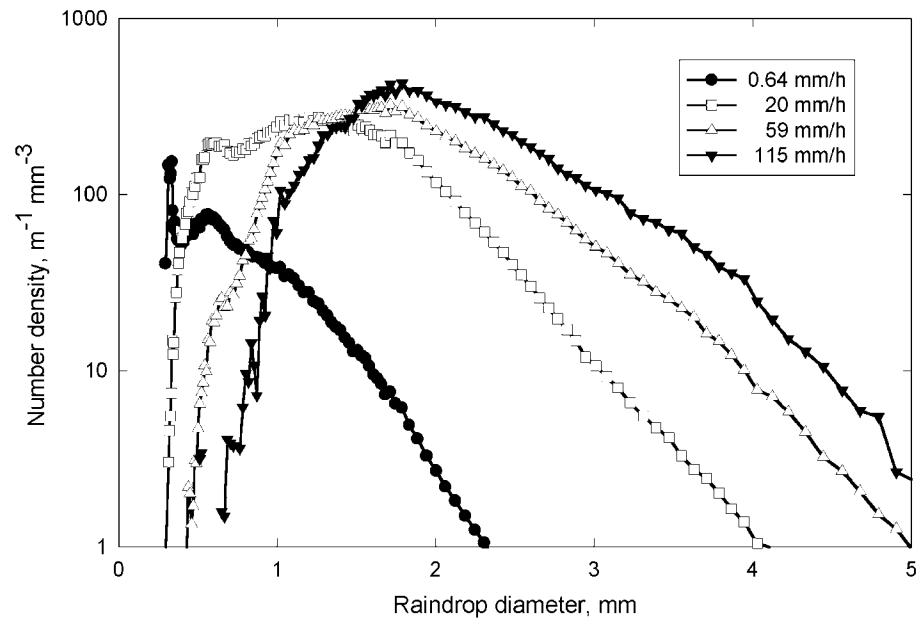

Figure 2b. Drop size density versus drop diameter, for four different categories (0–10, 10–40, 40–100, and 100–160 mm h^{-1}) of rain rate. The data are from Singapore.

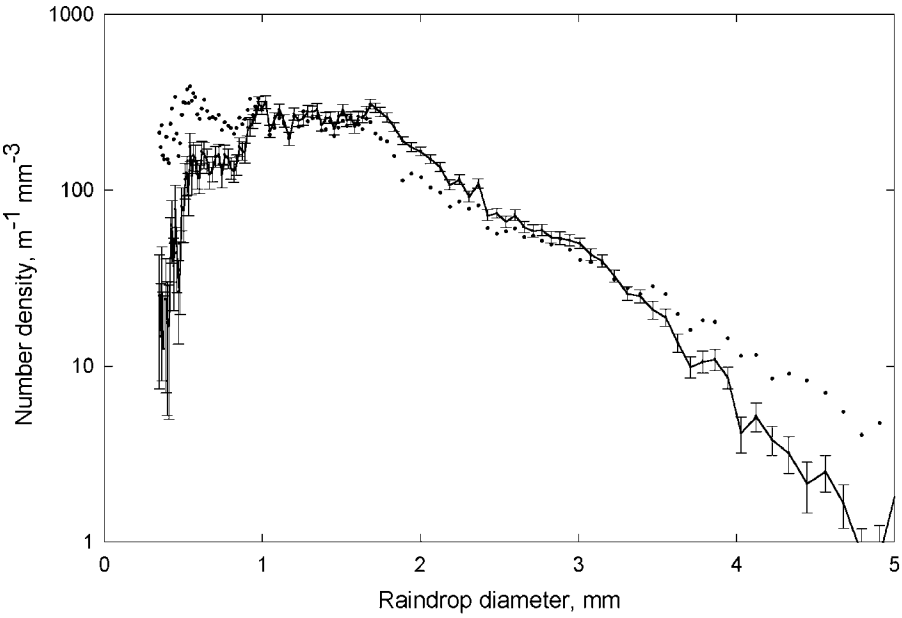

Figure 3a. Drop size density versus drop diameter, for rain rate category 40–50 mm h^{-1} (average 45 mm h^{-1}). The solid curve is the mean distribution, with standard deviations in the mean indicated by error bars, while the solid circles show the standard deviation. The data are from Chilbolton.

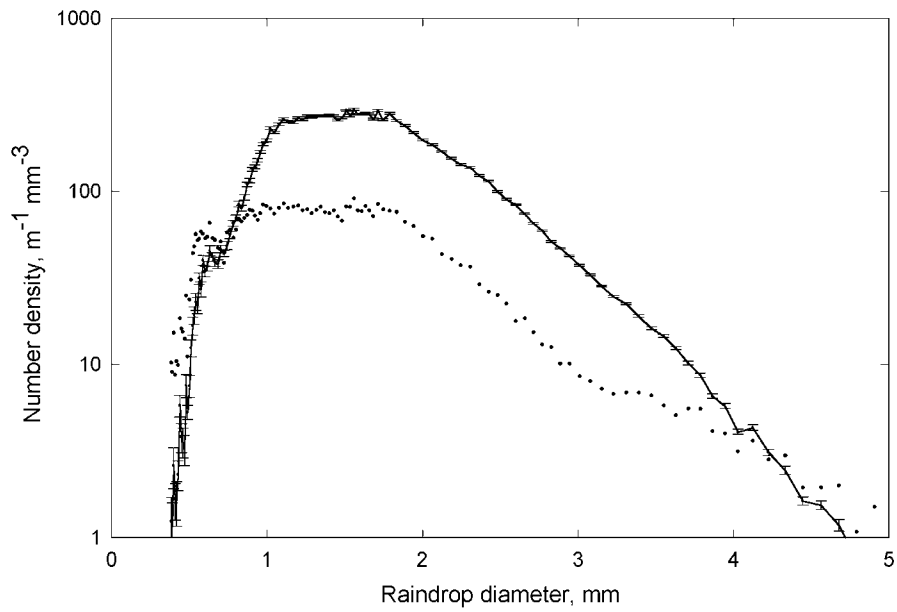

Figure 3b. Drop size density versus diameter, for rain rate category 40–50 mm h^{-1} (average 45 mm h^{-1}). The solid curve is the mean distribution, with standard deviation in the mean indicated by error bars, while the solid circles show the standard deviation. The data are from Singapore.

[12] These statistical calculations are useful for two reasons: First, an estimate can be made of the significance of the long-term DSDs obtained from different sites. Second, they enable an estimate of what size of spread might be expected for a single measurement.

5. Calculation of k and α

5.1. Derivation From DSDs

[13] Joss disdrometers with a collection area of 5000 mm^2 and an integration time of 10 s at Chilbolton and 30 s Singapore were used for data collection of DSDs. The reduced data matrix referred to in section 3 is used for the analysis.

[14] For each row of the matrix formed, the rain rate is calculated by summing the contributions to the total water content from all drop bins, assuming the drops to be spherical:

$$R_j = 0.096\pi \sum_{D_i} (D_i/2)^3 N_i, \qquad (1)$$

where R_j is the average rain rate (mm h^{-1}) of rain rate interval j, D_i is the mean drop diameter of bin number i of the disdrometer (mm), N_i is the average number of counts in bin number i, and the effects of area and integration time are incorporated in the constant 0.096. (For the Singapore matrix this equation is divided by 3.)

[15] For each row of the matrix formed, the theoretical attenuation at frequency f is calculated by summing the contributions to the specific attenuation from all drop bins. It is again assumed that drops are spherical, in order to apply the simple and exact Mie theory for scattering calculations. The specific attenuation is then

$$A_{j,f} = 4.343 \times 10^{-3} \sum_{D_i} C_f(D_i) N_i^V \quad \mathrm{dB/km}, \qquad (2)$$

where

$C_f(D_i)$ extinction cross section at frequency f (mm^2),
$N_i^V = N_i/v_i t A$ average number of drops per unit volume in bin number i (m^{-3}),
A disdrometer collection area,
t integration time,
v_i terminal velocity of drops in bin i.

Care must be taken when calculating N_i^V in order to correct for the different integration times at Chilbolton and Singapore, although the integration time is not relevant for further analyses once the matrix and vector are established using the correct integration time, provided it is the same for equations (1) and (2). Neither does it matter if the collection areas differ, since it is used in both equations.

Table 2. Values of k and α Found by Linear Regression of log ($A_{j,f}$) Against log (R_j).

Frequency, MHz	k, Chilbolton	k, Singapore	α, Chilbolton	α, Singapore
50	0.537	0.489	0.842	0.898
100	1.246	0.861	0.642	0.764
200	1.585	0.897	0.555	0.730
300	1.576	0.858	0.542	0.727
400	1.514	0.824	0.544	0.729

[16] The values of k and α in the specific attenuation relationship $\gamma = kR^\alpha$ are then found by linear regression of log ($A_{j,f}$) against log (R_j), where j refers to the category of rain rate. This procedure can be repeated for any frequency of interest. Table 2 gives the calculated values of k and α for 50, 100, 200, 300, and 400 MHz. For a more detailed investigation in a case where the uncertainty in drop size distributions is not the dominating uncertainty, a more accurate polarization-dependent calculation can be carried out. A model for the drop shape would then be used, together with a method such as T-matrix or point matching, in order to calculate the extinction coefficients C_f to be used, and k and α would then be polarization dependent, as given by *ITU-R* [1997].

5.2. Derivation From Logarithmic Regression on Measured Attenuation Against Rain Rate

[17] Estimates of the values of k and α can be derived from the measured values of attenuation at 57, 97, 135, and 210 GHz together with the simultaneous measurements of rain rate, taking linear regressions of log ($A_{j,f}$) against log (R_j), where j now refers to pairs of observed single observations. In the current study, only events with a peak rain rate of more than 50 mm h^{-1} have been considered, in order to ensure that a wide range of rain rates is represented in the analysis.

5.3. Results

[18] Figures 4a–4c show attenuations at rain rates of 10, 30, and 70 mm h^{-1}, respectively, as a function of frequency, using the values of k and α derived from measurements of attenuation at 57, 97, 135, and 210 GHz, from Chilbolton, together with curves showing the attenuations from the ITU model and those inferred from the DSDs measured at Chilbolton.

[19] From Figure 4a we see a marked underestimation of attenuation by the derived values of attenuation with respect to the experimental attenuation values. One

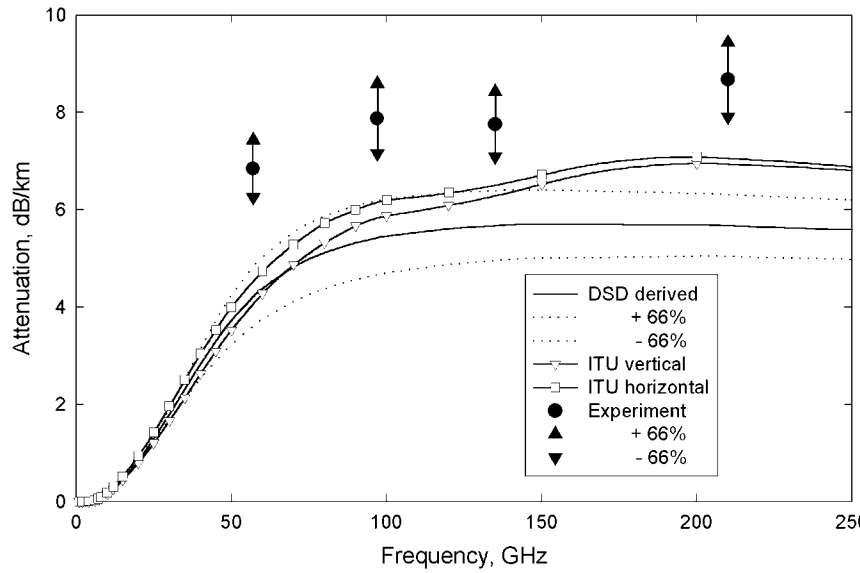

Figure 4a. Specific rain attenuation versus frequency, at 10 mm h^{-1}, calculated from (1) DSDs measured at Chilbolton, drawn together with their upper and lower 66% confidence limits and (2) *ITU-R* [1997] for vertical and horizontal polarization. Circles with upward and downward pointing arrows indicate values from measurements at 57, 97, 135, and 210 GHz with 66% confidence limits.

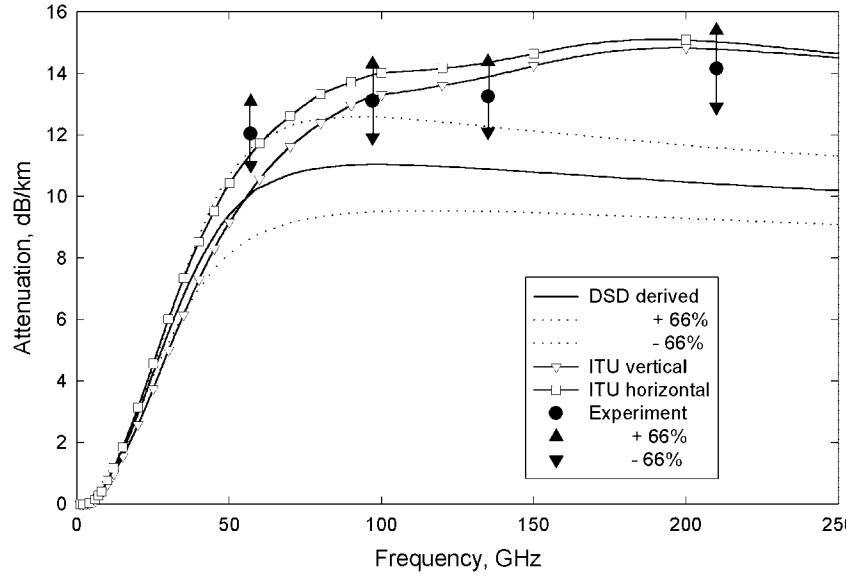

Figure 4b. As in Figure 4a, but for rain rate of 30 mm h^{-1}.

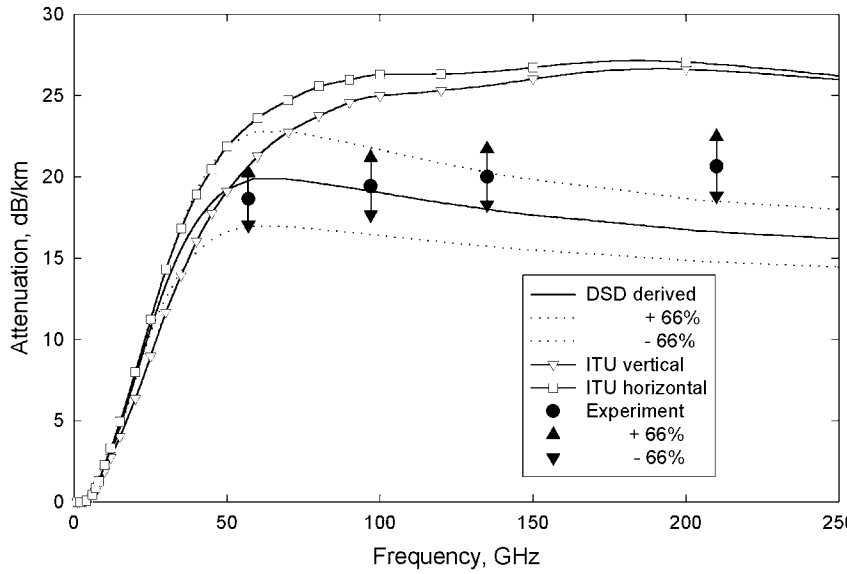

Figure 4c. As in Figure 4a, but for rain rate of 70 mm h^{-1}.

reason for the difference may be incorrect assumptions as to the number of raindrops in the air, for instance, due to wind, which reduces the effective collection area of rain gauges. Another reason may be the ability of the disdrometer to count the number of small raindrops, which will dominate at low rain rates.

[20] In general, from Figure 4a–4c, at high rain rates, it is apparent that the attenuations derived from the two separate methods (DSDs from Chilbolton and attenuation measurements from Chilbolton) agree quite well with each other but differ from the ITU values. At intermediate rain rates the attenuation measurements agree with the ITU curves, while at low rain rates the attenuations deduced from the DSDs agree with the ITU curves. At higher rain rates the ITU curves indicate higher attenuations than those either measured or deduced from measured DSDs.

[21] Figures 5a–5c compare the attenuations resulting from the DSDs measured in Singapore with those from Chilbolton. At all rain rates the Chilbolton and Singapore DSD data agree quite well with each other at frequencies up to about 40 GHz. At higher frequencies, however, differences start to become apparent. At the lower rain rates the Chilbolton DSDs indicate higher attenuations than do the Singapore DSDs, whereas at the intermediate and higher rain rates, the Chilbolton DSDs indicate lower attenuations.

6. Calculation of Parameters of Fitted Distributions

6.1. Fitted Distributions

[22] The impact-type disdrometer may not be sufficiently sensitive to small raindrops, but as shown in Figures 2a and 2b, the number of small raindrops is generally decreasing as the rain rate increases. In a paper by *Sheppard and Joe* [1994] the "dead time" of the RD-69 disdrometer was taken into account, in order to correct for the number of very small raindrops. The authors indicated that a negative exponential fit is appropriate. The "dead time" correction was attempted for the Chilbolton and Singapore data, but no significant difference was found, except perhaps for the lowest rain rates.

[23] Recently, *Jiang et al.* [1997] demonstrated very good fits of DSDs to Weibull and gamma distributions, while a shifted lognormal distribution has been suggested by *Park et al.* [1983]. The measured drop size distributions from Chilbolton and Singapore have therefore been fitted to these distributions, using a least squares regres-

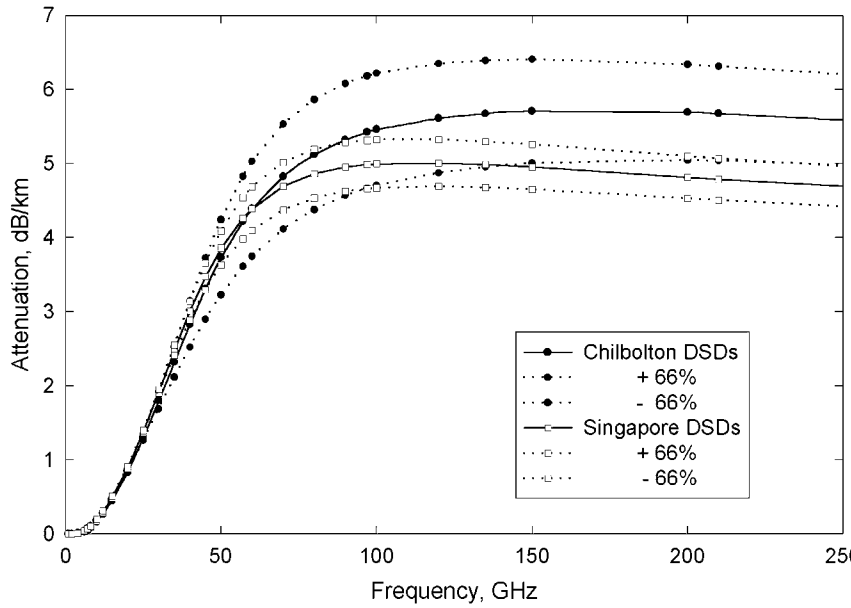

Figure 5a. Specific rain attenuation at 10 mm h^{-1} versus frequency, calculated from the Chilbolton DSDs and Singapore DSDs, together with their upper and lower 66% confidence limits.

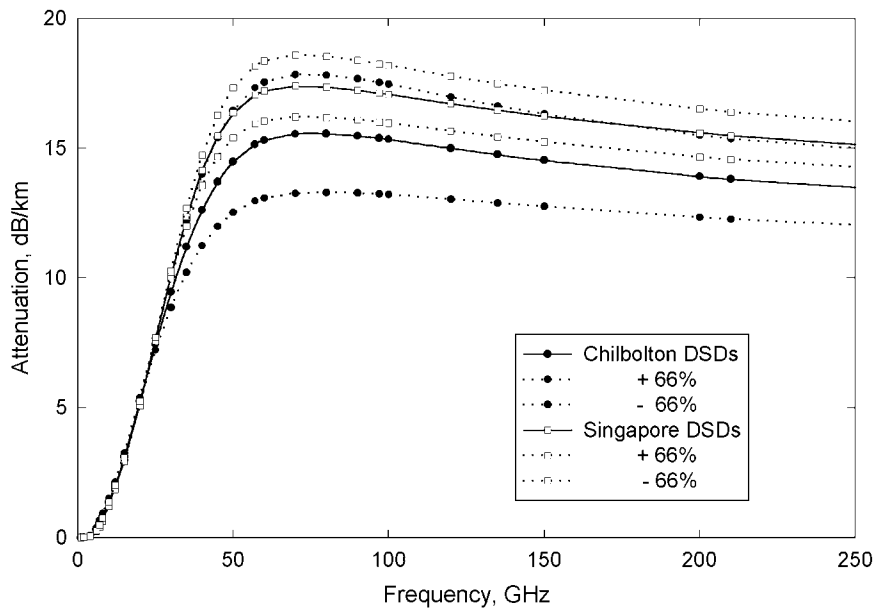

Figure 5b. As in Figure 5a, but for a rain rate of 50 mm h^{-1}.

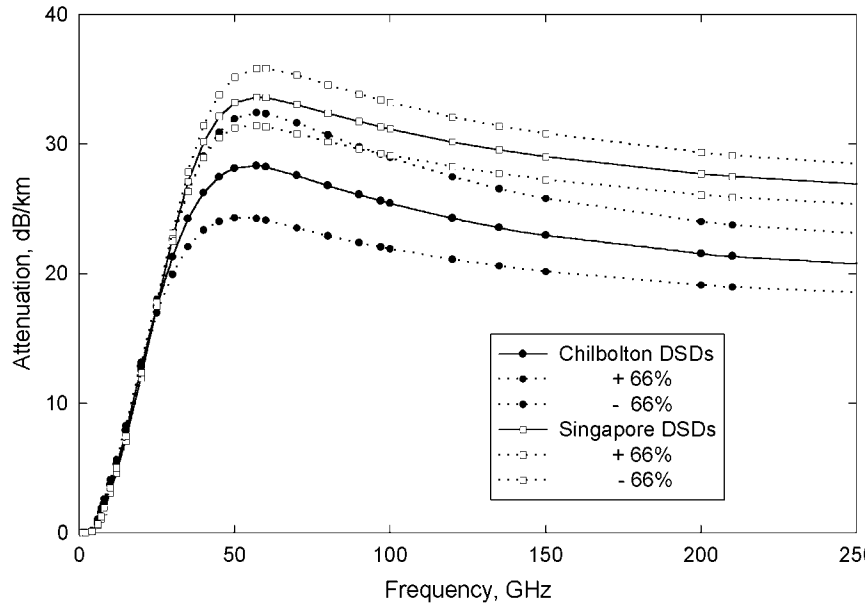

Figure 5c. As in Figure 5a, but for a rain rate of 110 mm h^{-1}.

sion procedure. The respective parameters are expressed as functions of rain rate, using the matrix described in section 3 with 3 years of averaged data. Both the Weibull and lognormal distributions were fitted to the drop density in units of mm^{-1} m^{-2} s^{-1}, although this may be transformed to drop density in units of m^{-3} mm^{-1} by dividing by the terminal drop velocity, as given, for example, by *Gunn and Kinzer* [1949].

[24] For the purpose of modeling attenuation the popular form of the shifted lognormal, gamma, and Weibull distributions for the drop diameters D can be written as follows:

Shifted lognormal

$$Y_{j,n} = N\frac{1}{(D+s)\sigma\sqrt{2\pi}}\exp\frac{-[\ln(D+s)-\mu]^2}{2\sigma 2}, \quad (3)$$

where s = 1 mm,

Weibull $$Y_{j,w} = N\frac{\eta}{\sigma}\left(\frac{D}{\sigma}\right)^{\eta-1}\exp\left\{-\left(\frac{D}{\sigma}\right)^{\eta}\right\}, \quad (4)$$

Gamma $$Y_{j,g} = N D^{n}\exp(-\Lambda D). \quad (5)$$

6.2. Results

[25] Figures 6a and 6b shows examples of how well the parameterized distributions fit the measured DSDs, for the Chilbolton and Singapore data, respectively. From this, it may be intuitively concluded that for the example shown, the lognormal distribution provides a better description for the DSD. However, a more quantitative figure of merit is the absolute value of the mean difference between the attenuation calculated from the original data and the attenuation calculated using modeled DSDs. Those distributions that give the smallest difference are considered "best." Thus Figures 7a and 7b indicate how well the Weibull, gamma, and lognormal distributions perform at different frequencies, at Chilbolton and Singapore, respectively. The plots are over an average of rain rates in the ranges observed for each site. From these graphs it can be seen that the lognormal distribution is the most successful in most cases, especially for the Singapore data.

[26] The gamma function does not, in general, provide a particularly good fit, even when setting n to a fixed value ($n = 2$). The main difference between the gamma fit and fitting to the other two distributions is that the gamma fit is performed on the drop density per unit volume, while the other two are fits to drop density per volume and velocity; that is, no assumption is made

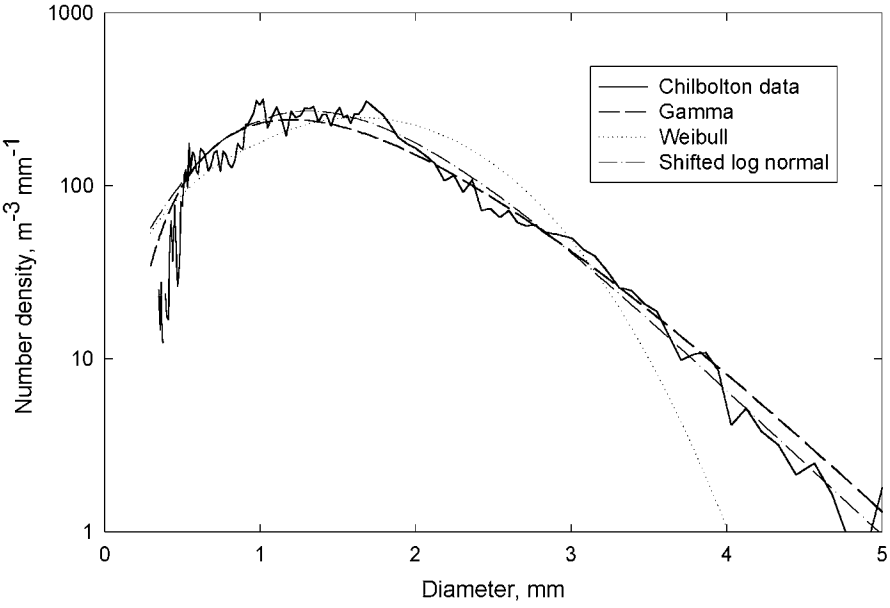

Figure 6a. Drop size density versus diameter, for the rain rate category 40–50 mm h^{-1} (average 45 mm h^{-1}). Data are for Chilbolton.

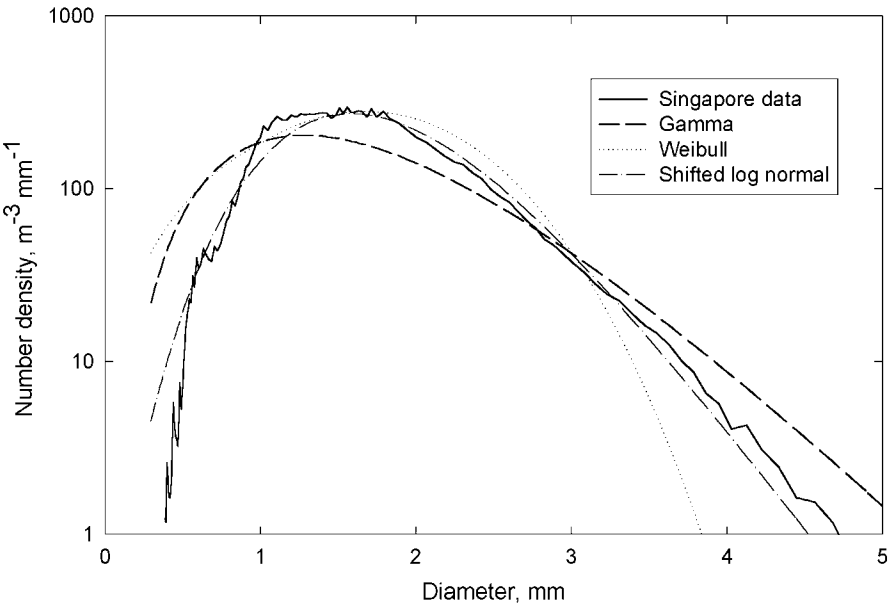

Figure 6b. Drop size density versus diameter, for rain rate category 40–50 mm h^{-1} (average 45 mm h^{-1}). Data are for Singapore.

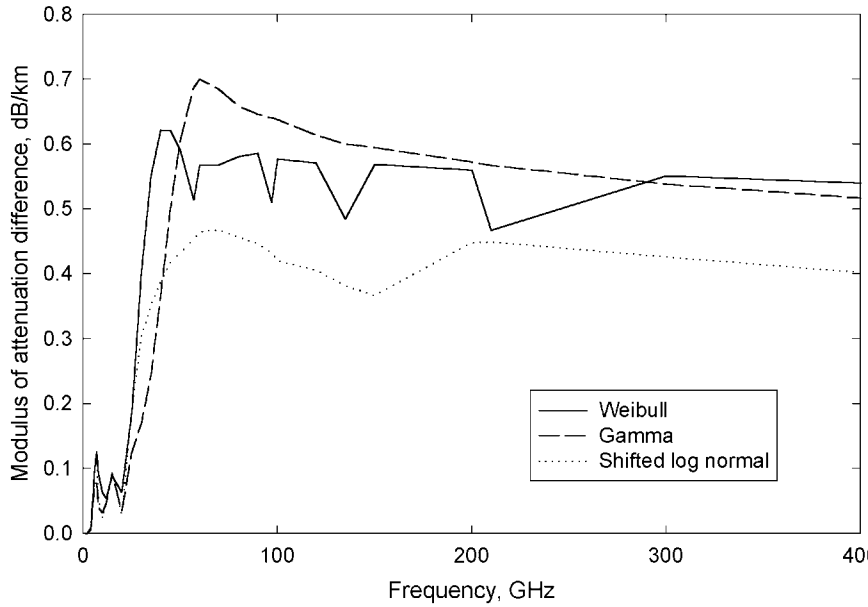

Figure 7a. Absolute value (modulus) of attenuation difference between calculated attenuation using measured DSDs and calculated attenuation using fitted DSDs, as a function of frequency. Data are for Chilbolton.

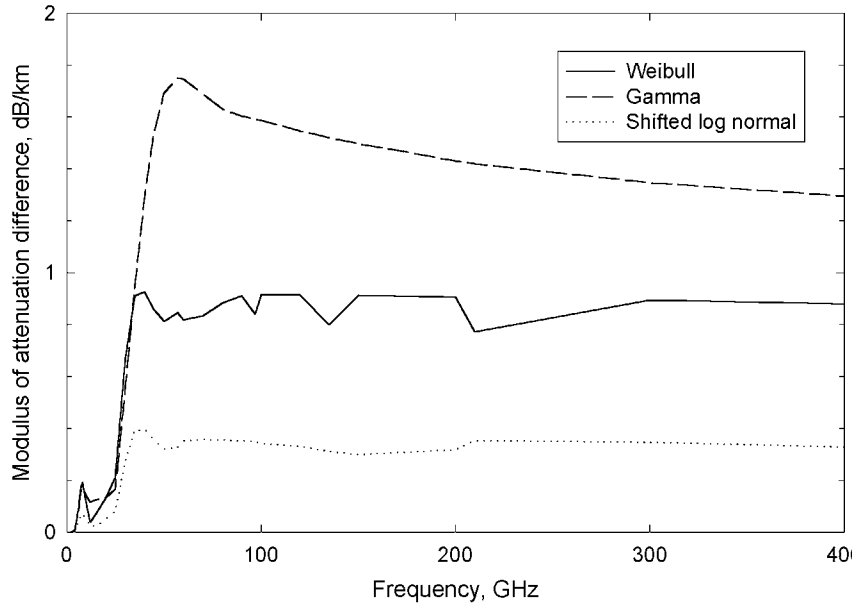

Figure 7b. Absolute value (modulus) of attenuation difference between calculated attenuation using measured DSDs and calculated attenuation using fitted DSDs, as a function of frequency. Data are for Singapore.

about the velocity distribution of raindrops. It is considered that functions that make no assumptions about the velocity of raindrops are more appropriate, especially since there may not always be agreement on the form of velocity function to be used. For the shifted lognormal and the Weibull distributions the closed rain-rate-dependent form of the distributions for Chilbolton and Singapore has been derived.

[27] The parameters of the shifted lognormal distribution, equation (3), are given by the following expressions:

$$\sigma_{n,\,\text{Chilbolton}} = 0.29,\ N_{n,\,\text{Chilbolton}} = 1287R^{0.2},$$

$$\mu_{n,\text{Chilbolton}} = 0.37R^{0.26},$$

$$\sigma_{n,\,\text{Singapore}} = 0.23,\ N_{n,\,\text{Singapore}} = 408R^{0.48},$$

$$\mu_{n,\text{Singapore}} = 0.59R^{0.15}.$$

The parameters of the Weibull distribution, equation (4), are

$$\sigma_{w,\,\text{Chilbolton}} = 0.65,\ R^{0.30},\ N_{w,\text{Chilbolton}} = 1180R^{0.23},$$

$$\eta_{w,\text{Chilbolton}} = 1.69R^{0.13},$$

$$\sigma_{w,\,\text{Singapore}} = 0.99\,R^{0.19},\ N_{w,\,\text{Singapore}} = 421R^{0.5},$$

$$\eta_{w,\,\text{Singapore}} = 2.15R^{0.1}.$$

The Singapore distribution is somewhat narrower than that for Chilbolton. This agrees with the theory of microphysics of precipitation, as explained in the introduction: Chilbolton has a dry inland climate, while Singapore is salty coastal.

7. Conclusions

[28] The main conclusion is that disdrometer measurements of raindrop size distributions taken over a long period of time can be used to derive frequency-independent basic parameters of importance to the modeling of rain attenuation. These parameters will vary with climatic conditions and levels of pollution, and it is therefore necessary to obtain DSD measurements from different sites around the world.

[29] Using the calibration suggested by the manufacturer of the RD-69 disdrometer, the measured distributions both from Chilbolton, England, and from Singapore have shown the multimodal behavior reported by many researchers. This behavior seems to disappear when a more detailed calibration is applied. The highly nonlinear behavior of the RD-69 disdrometer should therefore be considered when utilizing such data for detailed analyses.

[30] The current analysis of data from Chilbolton and Singapore has shown that large discrepancies in attenuation compared to the values given by *ITU-R* [1997] might be expected, especially at the higher frequencies. At frequencies up to 70 GHz, agreement with the ITU-R model is good. At higher frequencies and higher rain rates the results presented here indicate attenuations lower than those predicted by the ITU-R model. These discrepancies have been confirmed by attenuation measurements at the Chilbolton site, which have been conducted independently from the DSD measurements. Comparisons between attenuations derived from the DSDs measured at Chilbolton and Singapore further illustrate the possibility that a single, global DSD might not be appropriate for attenuation predictions.

[31] Fitting of measured drop size distributions to gamma, shifted lognormal, and Weibull distributions has shown that the shifted lognormal distribution performs most effectively in modeling the measured distributions, at most rain rate and frequency combinations. This is in agreement with the results reported by *Maitra and Gibbins* [1999]. The Weibull distribution performs almost as well in many cases, while the gamma distribution performs least effectively.

[32] **Acknowledgments.** The authors are grateful to Carron Wilson for access to the data from Singapore, to Jun Tan for assistance in checking extinction coefficient calculations, and to the reviewers for their helpful comments. Part of this work was supported by the Radiocommunications Agency, United Kingdom.

References

Gibbins, C. J., D. G. Carter, P. A. Eggett, K. A. Lidiard, M. G. Pike, M. A. Tracey, E. H. White, J. M. Woodroffe, and U. M. Yilmaz, A 500m experimental range for propagation studies at millimetre, infra-red and optical wavelengths, *J. Inst. Electron. Radio Eng.*, *57*, 227–234, 1987.

Gunn, R., and G. D. Kinzer, The terminal velocity of fall for water droplets in stagnant air, *J. Meteorol.*, *6*, 243–248, 1949.

International Telecommunication Union Radiocommunication Sector (ITU-R), Specific attenuation model for rain for use in prediction methods, *ITU-R Recomm. P.838*, Geneva, 1997.

Jiang, H., M. Sano, and M. Sekine, Weibull raindrop-size distribution and its application to rain attenuation, *IEE Proc., Part H: Microwaves Antennas Propag.*, *144*(3), 197–200, 1997.

Jones, D. M., A, Raindrop spectra at the ground, *J. Appl. Meteorol.*, *31*(10), 1219–1225, 1992.

Laws, J. O., and D. A. Parsons, The relation of raindrop-size to intensity, *Eos Trans. AGU*, *24*, 452–460, 1943.

List, R., and G. M. McFarquhar, The role of breakup and coa-

lescence in the three-peak equilibrium distribution of raindrops, *J. Atmos. Sci.*, *47*(19), 2274–2292, 1990.

Maitra, A., and C. J. Gibbins, Modelling of raindrop size distributions from multiwavelength rain attenuation measurements, *Radio Sci.*, *34*(3), 657–666, 1999.

Marshall, J. S., and W. M. Palmer, The distribution of raindrops with size, *J. Meteorol.*, *5*, 165–166, 1948.

McFarquhar, G., and R. List, The effect of curve fits for the disdrometer calibration on raindrop spectra, rainfall rate, and radar reflectivity, *J. Appl. Meteorol.*, *32*, 774–782, 1993.

Park, S. W., J. K. Mitchell, and G. D. Bubenzer, Rainfall characteristics and their relation to splash erosion, *Trans. ASAE*, *26*(3), 795–804, 1983.

Rogers, R. R., and M. K. Yau, *A Short Course in Cloud Physics*, Butterworth-Heinemann, Woburn, Mass., 1989.

Sheppard, B. E., Effect of irregularities in the diameter classification of raindrops by the Joss-Waldvogel disdrometer, *J. Atmos. Oceanic Technol.*, *7*, 180–183, 1990.

Sheppard, B. E., and P. I. Joe, Comparison of raindrop size distribution measurements by Joss-Waldvogel distrometer, a PMS 2 DG spectrometer, and a POSS Doppler radar, *J. Atmos. Oceanic Technol.*, *11*, 874–887, 1994.

Steiner, M., and A. Waldvogel, Peaks in raindrop size distributions, *J. Atmos. Sci.*, *44*(20), 3127–3133, 1987.

Ugai, S., K. Kato, M. Nishijima, T. Kan, and K. Tazaki, Fine structure of rainfall, *Ann. Telecommunic.*, *32*(11–12), 422–429, 1997.

Wilson, C. L., J. W. F. Goddard, and D. N. Ladd, Distrometer derived *Z-R* relatioships in Singapore and Papua New Guinea, and implications for the TRMM products, paper presented at 29th Conference on Radar Meteorology, Am. Meteorol. Soc., Montreal, Canada, July 1999.

W. Åsen, Norwegian Post and Telecommunications Authority, P. O. Box 447, N-0104 Oslo, Norway. (walther.asen@npt.no)

C. J. Gibbins, Radio Communications Research Unit, Rutherford Appleton Laboratory, Chilton, Didcot, Oxfordshire OX11 0QX, England, UK. (c.j.gibbins@rl.ac.uk)